EncoderMI: Membership Inference against Pre-trained Encoders in Contrastive Learning

Hongbin Liu*
Duke University
hongbin.liu@duke.edu

Jinyuan Jia*
Duke University
jinyuan.jia@duke.edu

Wenjie Qu†
Huazhong University of Science and Technology
wenjiequ@hust.edu.cn

Neil Zhenqiang Gong
Duke University
neil.gong@duke.edu

ABSTRACT

Given a set of unlabeled images or (image, text) pairs, *contrastive learning* aims to pre-train an *image encoder* that can be used as a feature extractor for many downstream tasks. In this work, we propose *EncoderMI*, the first *membership inference* method against image encoders pre-trained by contrastive learning. In particular, given an input and a black-box access to an image encoder, EncoderMI aims to infer whether the input is in the training dataset of the image encoder. EncoderMI can be used 1) by a data owner to audit whether its (public) data was used to pre-train an image encoder without its authorization or 2) by an attacker to compromise privacy of the training data when it is private/sensitive. Our EncoderMI exploits the *overfitting* of the image encoder towards its training data. In particular, an overfitted image encoder is more likely to output more (or less) similar feature vectors for two augmented versions of an input in (or not in) its training dataset. We evaluate EncoderMI on image encoders pre-trained on multiple datasets by ourselves as well as the Contrastive Language-Image Pre-training (CLIP) image encoder, which is pre-trained on 400 million (image, text) pairs collected from the Internet and released by OpenAI. Our results show that EncoderMI can achieve high *accuracy*, *precision*, and *recall*. We also explore a countermeasure against EncoderMI via preventing overfitting through early stopping. Our results show that it achieves trade-offs between accuracy of EncoderMI and utility of the image encoder, i.e., it can reduce the accuracy of EncoderMI, but it also incurs classification accuracy loss of the downstream classifiers built based on the image encoder.

CCS CONCEPTS

• **Security and privacy**; • **Computing methodologies → Machine learning**;

KEYWORDS

Membership inference; contrastive learning; privacy-preserving machine learning

ACM Reference Format:
Hongbin Liu*, Jinyuan Jia*, Wenjie Qu†, and Neil Zhenqiang Gong. 2021. EncoderMI: Membership Inference against Pre-trained Encoders in Contrastive Learning. In *Proceedings of the 2021 ACM SIGSAC Conference on Computer and Communications Security (CCS ’21), November 15–19, 2021, Virtual Event, Republic of Korea.* ACM, New York, NY, USA, 15 pages. https://doi.org/10.1145/3460120.3484749

1 INTRODUCTION

Contrastive learning [10, 17, 20, 37, 38] is a promising approach for general-purpose AI. In particular, given an unlabeled dataset (called *pre-training dataset*) of images or (image, text) pairs, contrastive learning pre-trains an *image encoder* that can be used as a feature extractor for many downstream tasks. Given the image encoder, the downstream tasks require only a small amount of or no labeled training data. The pre-training of encoders, however, usually consumes a lot of data and computation resources. Therefore, typically, a powerful encoder provider (e.g., OpenAI, Google) pre-trains encoders and then provides service to downstream customers (e.g., less resourceful organizations, end users).

Existing studies [10, 20, 38] on contrastive learning mainly focus on how to train a better image encoder such that it can achieve better performance on the downstream tasks. The security and privacy of contrastive learning, however, is largely unexplored. In this work, we perform the first systematic study on *membership inference* against image encoders pre-trained by contrastive learning. In particular, we aim to infer whether an input image is in the pre-training dataset of an image encoder. An input is called a *member* (or *non-member*) of an image encoder if it is in (or not in) the pre-training dataset of the image encoder.

Membership inference in contrastive learning has two important applications. Suppose data owners make their images public on the Internet, e.g., on Twitter. An AI company (e.g., OpenAI) collects and uses the public data to pre-train and monetize image encoders without the data owners’ authorization. Such practices may violate the data owners’ data security. For instance, Twitter asked Clearview to stop taking public images from its website for model training [1]; and FTC requires Ever to delete models trained on unauthorized user data [3]. The first application of membership inference is that a data owner can use a membership inference method to audit whether his/her (public) data was used to pre-train image encoders

*The first two authors made equal contributions.
†Wenjie Qu performed this research when he was a remote intern in Gong’s group.

CCS ’21, November 15–19, 2021, Virtual Event, Republic of Korea.
© 2021 Association for Computing Machinery.
ACM ISBN 978-1-4503-8454-4/21/11…$15.00
https://doi.org/10.1145/3460120.3484749

without his/her authorization, though the membership inference result may not have formal guarantees. The second application of membership inference is that an attacker can use it to compromise privacy of the pre-training data when it is private/sensitive. For instance, hospitals may collaboratively use contrastive learning to pre-train image encoders that can be shared across hospitals to solve various downstream healthcare tasks, e.g., lung CT image based COVID-19 testing [16] and skin disease prediction. In such cases, the pre-training data may include sensitive medical images and one hospital may infer other hospitals' sensitive members of the image encoder.

Existing membership inference methods [29, 34, 35, 42, 44, 48] are mainly designed for classifiers. For example, given the confidence score vector outputted by a classifier for an input, they aim to infer whether the input is in the training dataset of the classifier. The idea of existing membership inference methods [42, 44] is to exploit the *overfitting* of the classifier. For instance, the confidence score vectors of members and non-members of a classifier are statistically distinguishable. Therefore, the confidence score vector outputted by the classifier for an input can capture whether the input is a member of the classifier. However, given an input, an image encoder outputs a feature vector for it. The feature vector itself does not capture the overfitting of the image encoder on the input. As shown by our experimental results in Section 5.2, existing membership inference methods for classifiers are close to random guessing when generalized to infer the members of an image encoder.

Our work: In this work, we propose EncoderMI, the first membership inference method against contrastive learning.

Threat model. We call an entity (e.g., a data owner, an attacker) who performs membership inference an *inferrer*. We assume an inferrer has a black-box access to a pre-trained image encoder (called *target encoder*), which is the most difficult and general scenario. The inferrer aims to infer whether an input is in the pre-training dataset of the target encoder. The pre-training of an image encoder relies on three key dimensions: *pre-training data distribution*, *encoder architecture*, and *training algorithm*. In other words, we have three dimensions of background knowledge. The inferrer may or may not know each of them. Therefore, we have eight different types of background knowledge for the inferrer in total. In our methods, we assume the inferrer has a *shadow dataset*. In particular, the shadow dataset could have the same distribution as the pre-training data distribution if the inferrer knows it. Otherwise, we assume the shadow dataset has a different distribution from the pre-training dataset. Moreover, if the inferrer does not know the encoder architecture (or training algorithm), we consider the inferrer can assume one and perform membership inference based on the assumed one.

Our EncoderMI. An important module in contrastive learning is *data augmentation*. Roughly speaking, given an input, the data augmentation module creates another random input (called *augmented input*) via applying a sequence of random operations (e.g., random grayscale, random resized crop) to the input. We observe that contrastive learning essentially aims to pre-train an image encoder such that it outputs similar feature vectors for two augmented inputs created from the same input. EncoderMI is based on this observation. Specifically, when an image encoder is *overfitted* to its pre-training dataset, it may output more (or less) similar feature vectors for augmented inputs that are created from an input in (or not in) the pre-training dataset. In EncoderMI, an inferrer builds a binary classifier (called *inference classifier*) to predict whether an input is a member of the target encoder. Roughly speaking, our inference classifier predicts an input to be a member of the target encoder if the target encoder produces similar feature vectors for the augmented inputs created from the input. Next, we discuss how to build inference classifiers.

Given a shadow dataset, we first split it into two subsets, namely, *shadow member dataset* and *shadow non-member dataset*. Then, we pre-train an encoder (called *shadow encoder*) using the shadow member dataset based on the background knowledge of the inferrer (e.g., the inferrer can adopt the same encoder architecture and training algorithm used to pre-train the target encoder if he/she knows them). Given the shadow encoder and the shadow dataset, we extract *membership features* for each input in the shadow dataset. In particular, given an input in the shadow dataset, we first create n augmented inputs via the data augmentation module of the training algorithm used to train the shadow encoder, then use the shadow encoder to produce a feature vector for each augmented input, and finally compute the set of $n \cdot (n-1)/2$ pairwise similarity scores between the n feature vectors using a similarity metric as the membership features for the input. Given these membership features, we construct an *inference training dataset* via labeling the membership features as "member" (or "non-member") if they are created from an input that is in the shadow member (or non-member) dataset. Given the inference training dataset, we build an inference classifier to infer the members of the target encoder. We consider three types of classifiers: *vector-based classifier*, *set-based classifier*, and *threshold-based classifier*. Given an input and a black-box access to the target encoder, we first extract membership features for the input and then use an inference classifier to predict whether the input is a member of the target encoder.

Evaluation. To evaluate EncoderMI, we first conduct experiments on CIFAR10, STL10, and Tiny-ImageNet datasets via pre-training image encoders by ourselves. Our experimental results show that EncoderMI can achieve high *accuracy*, *precision*, and *recall* under all the eight different types of background knowledge. For instance, our vector-based inference classifier can achieve 88.7% – 96.5% accuracy on Tiny-ImageNet under the eight types of background knowledge. Moreover, EncoderMI can achieve higher accuracy as the inferrer has access to more background knowledge. We also apply EncoderMI to infer members of the CLIP's image encoder released by OpenAI [38]. In particular, we collect some *potential members* and ground truth non-members of the CLIP's image encoder from Google image search and Flickr. Our results show that EncoderMI is effective even if the inferrer does not know the pre-training data distribution, the encoder architecture, and the training algorithm of the CLIP's image encoder.

Countermeasure. When a data owner uses EncoderMI to audit data misuse, an encoder provider may adopt a countermeasure against EncoderMI to evade auditing. When an attacker uses EncoderMI to compromise pre-training data privacy, a countermeasure can be adopted to enhance privacy. As EncoderMI exploits the overfitting of the target encoder on its training data, we can leverage countermeasures that prevent overfitting. In particular, we generalize early stopping [47], a state-of-the-art overfitting-prevention-based countermeasure against membership inference to classifiers, to mitigate membership inference to pre-trained encoders. Roughly speaking, the idea of early stopping is to train the target encoder with less number of epochs to prevent overfitting. Our results show that it achieves trade-offs between the accuracy of EncoderMI and the utility of the target encoder. More specifically, it can reduce the accuracy of our EncoderMI, but it also incurs classification accuracy loss of the downstream classifiers built based on the target encoder.

In summary, we make the following contributions in this work:

- We propose EncoderMI, the first membership inference method against contrastive learning.
- We conduct extensive experiments to evaluate our EncoderMI on CIFAR10, STL10, and Tiny-ImageNet datasets. Moreover, we apply EncoderMI to CLIP's image encoder.
- We evaluate an early stopping based countermeasure against EncoderMI. Our results show that it achieves trade-offs between accuracy of EncoderMI and utility of the encoder.

2 BACKGROUND ON CONTRASTIVE LEARNING

Given a large amount of unlabeled images or (image, text) pairs (called *pre-training dataset*), contrastive learning aims to pre-train a neural network (called *image encoder*) that can be used as a feature extractor for many downstream tasks (e.g., image classification). Given an input image, the pre-trained image encoder outputs a *feature vector* for it.

2.1 Pre-training an Encoder

An essential module in contrastive learning is *data augmentation*. Given an input image, the data augmentation module can create another random input (called *augmented input*) by a sequence of random operations such as random grayscale, random resized crop, etc.. An augmented input and the original input have the same size. Moreover, we can create multiple augmented inputs for each input using the data augmentation module. Roughly speaking, the idea of contrastive learning is to pre-train an image encoder such that it outputs similar (or dissimilar) feature vectors for two augmented inputs created from the same (or different) input(s). Contrastive learning formulates such similarity as a *contrastive loss*, which an image encoder is trained to minimize. Next, we introduce three popular contrastive learning algorithms, i.e., MoCo [20], SimCLR [10], and CLIP [38], to further illustrate the idea of contrastive learning.

MoCo [20]: MoCo pre-trains an image encoder on unlabeled images. There are three major modules in MoCo: an *image encoder* (denoted as h), a *momentum encoder* (denoted as h_m), and a *dictionary* (denoted as Γ). The image encoder outputs a feature vector for an input or an augmented input. The momentum encoder has the same architecture with the image encoder, but is updated much more slowly compared with the image encoder. Given an input or an augmented input, the momentum encoder also outputs a vector for it. To distinguish with feature vector, we call it *key vector*. The *dictionary* module maintains a queue of key vectors outputted by the momentum encoder for augmented inputs created from inputs in previous several mini-batches. Moreover, the dictionary is dynamically updated during the pre-training of the image encoder.

Given a mini-batch of N inputs, MoCo creates two augmented inputs for each input in the mini-batch. The two augmented inputs are respectively passed to the image encoder and the momentum encoder. For simplicity, we use $\mathbf{u}_i$ and $\mathbf{u}_j$ to denote these two augmented inputs. Given the two augmented inputs, the image encoder h, the momentum encoder h_m, and the dictionary Γ, MoCo defines a contrastive loss as follows:

$$\begin{aligned}&\ell(\mathbf{u}_i)\\&=-\log\Big(\frac{exp(sim(h(\mathbf{u}_i),h_m(\mathbf{u}_j))/\tau)}{exp(sim(h(\mathbf{u}_i),h_m(\mathbf{u}_j))/\tau)+\sum\limits_{\mathbf{z}\in\Gamma}exp(sim(h(\mathbf{u}_i),\mathbf{z})/\tau)}\Big),\end{aligned} \tag{1}$$

where exp is the natural exponential function, sim computes cosine similarity between two vectors, and τ represents a temperature parameter. The final contrastive loss is summed over the contrastive loss $\ell(\mathbf{u}_i)$ of the N augmented inputs (i.e., u_i's) corresponding to the N inputs. MoCo pre-trains the image encoder via minimizing the final contrastive loss. Finally, the N key vectors (i.e., $h_m(\mathbf{u}_j)$'s) outputted by the momentum encoder for the N augmented inputs (i.e., u_j's) are enqueued to the dictionary while the N key vectors from the "oldest" mini-batch are dequeued.

SimCLR [10]: Similar to MoCo [20], SimCLR also tries to pre-train an image encoder on unlabeled images. Given a mini-batch of N inputs, SimCLR creates two augmented inputs for each input in the mini-batch via data augmentation. Given $2 \cdot N$ augmented inputs (denoted as $\{\mathbf{u}_1, \mathbf{u}_2, \cdots, \mathbf{u}_{2\cdot N}\}$), SimCLR aims to pre-train the image encoder such that it outputs similar (or dissimilar) feature vectors for two augmented inputs that are created from the same (or different) input(s). Formally, given a pair $(\mathbf{u}_i, \mathbf{u}_j)$ of augmented inputs created from the same input, the contrastive loss is defined as follows:

$$\ell_{ij}=-\log\Big(\frac{exp(sim(g(h(\mathbf{u}_i)),g(h(\mathbf{u}_j)))/\tau)}{\sum_{k=1}^{2\cdot N}\mathbb{I}(k\neq i)\cdot exp(sim(g(h(\mathbf{u}_i)),g(h(\mathbf{u}_k)))/\tau)}\Big), \tag{2}$$

where $\mathbb{I}$ is an indicator function, exp is the natural exponential function, sim computes cosine similarity between two vectors, h is the image encoder, g is the projection head, and τ is a temperature parameter. The final contrastive loss is summed over the contrastive loss ℓ_{ij} of all $2 \cdot N$ pairs of augmented inputs, where each input corresponds to two pairs of augmented inputs $(\mathbf{u}_i, \mathbf{u}_j)$ and $(\mathbf{u}_j, \mathbf{u}_i)$. SimCLR pre-trains the image encoder via minimizing the final contrastive loss.

CLIP [38]: CLIP jointly pre-trains an image encoder and a text encoder on unlabeled (image, text) pairs. In particular, the text encoder takes a text as input and outputs a feature vector for it. Given a mini-batch of N (image, text) pairs, CLIP creates an augmented input image from each input image. For each augmented input image, CLIP forms a correct (image, text) pair using the augmented input image and the text that originally pairs with the input image from which the augmented input image is created, and CLIP forms $(N-1)$ incorrect pairs using the augmented input image and the remaining $(N-1)$ texts. Therefore, there are N correct pairs and $N \cdot (N-1)$ incorrect pairs in total. CLIP jointly pre-trains an image encoder and a text encoder such that, for a correct (or incorrect) pair of (image, text), the feature vector outputted by the image encoder for the augmented input image is similar (or dissimilar) to the feature vector outputted by the text encoder for the text.

Observation: We observe that these contrastive learning algorithms try to pre-train an image encoder that outputs similar feature vectors for two augmented inputs that are created from the same input. Specifically, we can have this observation for MoCo [20] and SimCLR [10] based on the definitions of their contrastive losses. For CLIP, given an (image, text) pair, the feature vector outputted by the image encoder for an augmented version of the image is similar to the feature vector outputted by the text encoder for the text. Therefore, the feature vectors outputted by the image encoder for two augmented inputs created from the input image are similar since both of them are similar to the feature vector outputted by the text encoder for the given text. As we will discuss in Section 4, our EncoderMI leverages this observation to infer members of an image encoder's pre-training dataset.

2.2 Training Downstream Classifiers

The image encoder can be used as a feature extractor for many downstream tasks. We consider the downstream task to be image classification in this work. In particular, suppose we have a labeled dataset (called *downstream dataset*). We first use the image encoder to extract feature vectors for inputs in the downstream dataset. Then, we follow the standard supervised learning to train a classifier (called *downstream classifier*) using the extracted feature vectors as well as the corresponding labels. Given a testing input from the downstream task, we first use the image encoder to extract the feature vector for it and then use the downstream classifier to predict a label for the extracted feature vector. The predicted label is viewed as the prediction result for the testing input.

3 PROBLEM FORMULATION

3.1 Threat Model

Inferrer's goal: Given an input image $\mathbf{x}$, an inferrer aims to infer whether it is in the pre-training dataset of an image encoder (called *target encoder*). We call an input a *member* of the target encoder if the input is in its pre-training dataset, otherwise we call the input a *non-member*. The inferrer aims to achieve high accuracy at inferring the members/non-members of the target encoder.

Inferrer's background knowledge: We consider an inferrer has a *black-box* access to the target encoder. We note that this is the most difficult and general scenario for the inferrer. A typical application scenario is that the encoder provider pre-trains an encoder and then provides an API to downstream customers. The pre-training of an encoder depends on three key dimensions, i.e., *pre-training data distribution*, *encoder architecture*, and *training algorithm* (e.g., MoCo, SimCLR). Therefore, we characterize the inferrer's background knowledge along these three dimensions.

- **Pre-training data distribution.** This background knowledge characterizes whether the inferrer knows the distribution of the pre-training dataset of the target encoder. In particular, if the inferrer knows the distribution, we assume he/she has access to a *shadow dataset* that has the same distribution as the pre-training dataset. Otherwise, we assume the inferrer has access to a shadow dataset that has a different distribution from the pre-training dataset. Note that, in both cases, we consider the shadow dataset does not have overlap with the pre-training dataset. For simplicity, we use $\mathcal{P}$ to denote this dimension of background knowledge.
- **Encoder architecture.** The inferrer may or may not know the architecture of the target encoder. When the inferrer does not know the target-encoder architecture, the inferrer can assume one and perform membership inference based on the assumed one. For instance, when the target encoder uses ResNet architecture, the inferrer may assume VGG architecture when performing membership inference. We use $\mathcal{E}$ to denote this dimension of background knowledge.
- **Training algorithm.** This dimension characterizes whether the inferrer knows the contrastive learning algorithm used to train the target encoder. When the inferrer does not know the training algorithm, the inferrer can perform membership inference based on an assumed one. For instance, when the training algorithm of the target encoder is MoCo [20], the inferrer may perform membership inference by assuming the training algorithm is SimCLR [10]. We use $\mathcal{T}$ to denote this dimension of background knowledge.

We use a triplet $\mathcal{B} = (\mathcal{P}, \mathcal{E}, \mathcal{T})$ to denote the three dimensions of the inferrer's background knowledge. Each dimension in $\mathcal{B}$ can be "yes" or "no", where a dimension is "yes" (or "no") when the corresponding dimension of background knowledge is available (or unavailable) to the inferrer. Therefore, we have eight different types of background knowledge in total. For instance, the inferrer knows the pre-training data distribution, architecture of the target encoder, and/or training algorithm when the encoder provider makes them public to increase transparency and trust.

Inferrer's capability: An inferrer can query the target encoder for the feature vector of any input or an augmented input.

3.2 Membership Inference

Given the inferrer's goal, background knowledge, and capability, we define our membership inference against contrastive learning as follows:

Definition 3.1 (Membership Inference against Contrastive Learning). Given a black-box access to a target encoder, the background knowledge $\mathcal{B} = (\mathcal{P}, \mathcal{E}, \mathcal{T})$, and an input, membership inference aims to infer whether the input is in the pre-training dataset of the target encoder.

4 OUR METHOD

4.1 Overview

Recall that a target encoder is trained to output similar feature vectors for the augmented versions of an input in the pre-training dataset. Our EncoderMI is based on this observation. Specifically, when an encoder is *overfitted* to its pre-training dataset, the encoder may output more (or less) similar feature vectors for augmented inputs created from an input in (or not in) the pre-training dataset. Therefore, our EncoderMI infers an input to be a member of the target encoder if the target encoder produces similar feature vectors for the augmented versions of the input. Specifically, in EncoderMI, an inferrer builds a binary classifier (called *inference classifier*), which predicts member/non-member for an input based on some features we create for the input. To distinguish with the feature vectors produced by the target encoder, we call the features used by the inference classifier *membership features.* Our membership features of an input are based on the similarity scores between the feature vectors of the input's augmented versions produced by the target encoder. Building our inference classifier requires a training dataset (called *inference training dataset*) which consists of known members and non-members. To construct an inference training dataset, we split the inferrer's shadow dataset into two subsets, which we call *shadow member dataset* and *shadow non-member dataset*, respectively. Then, the inferrer pre-trains an encoder (called *shadow encoder*) using the shadow member dataset. We construct an inference training dataset based on the shadow encoder and shadow dataset. Specifically, each input in the shadow member (or non-member) dataset is a member (or non-member) of the shadow encoder, and we create membership features for each input in the shadow dataset based on the shadow encoder. After building an inference classifier based on the inference training dataset, we apply it to infer members/non-members of the target encoder.

4.2 Building Inference Classifiers

We first introduce how to train a shadow encoder on a shadow dataset. Then, we discuss how to extract membership features for an input. Finally, we discuss how to construct an inference training dataset based on the shadow encoder and the shadow dataset, and given the constructed inference training dataset, we discuss how to build inference classifiers.

Training a shadow encoder: The first step of our EncoderMI is to train a shadow encoder whose ground truth members/non-members are known to the inferrer. For simplicity, we use $\tilde{h}$ to denote the shadow encoder. In particular, the inferrer splits its shadow dataset $\mathcal{D}_s$ into two non-overlapping subsets: shadow member dataset (denoted as $\mathcal{D}_s^m$) and shadow non-member dataset (denoted as $\mathcal{D}_s^{nm}$). Then, the inferrer pre-trains a shadow encoder using the shadow member dataset $\mathcal{D}_s^m$. If the inferrer has access to the target encoder's architecture (or training algorithm), the inferrer uses the same architecture (or training algorithm) for the shadow encoder, otherwise the inferrer assumes an architecture (or training algorithm) for the shadow encoder. We note that each input in the shadow member (or non-member) dataset is a member (or non-member) of the shadow encoder.

Extracting membership features: For each input in the shadow dataset, we extract its membership features based on the shadow encoder $\tilde{h}$. Our membership features are based on the key observation that an encoder (e.g., target encoder, shadow encoder) pre-trained by contrastive learning produces similar feature vectors for augmented versions of an input in the encoder's pre-training dataset. Therefore, given an input $\mathbf{x}$, we first create n augmented inputs using the data augmentation module $\mathcal{A}$ of the training algorithm used to pre-train the shadow encoder. We denote the n augmented inputs as $\mathbf{x}^1, \mathbf{x}^2, \cdots, \mathbf{x}^n$. Then, we use the shadow encoder to produce a feature vector for each augmented input. We denote by $\tilde{h}(\mathbf{x}^i)$ the feature vector produced by the shadow encoder $\tilde{h}$ for the augmented input $\mathbf{x}^i$, where $i = 1, 2, \cdots, n$. Our *membership features* for the input $\mathbf{x}$ consist of the set of pairwise similarity scores between the n feature vectors. Formally, we have:

$$\mathcal{M}(\mathbf{x}, \tilde{h}) = \{S(\tilde{h}(\mathbf{x}^i), \tilde{h}(\mathbf{x}^j))|i \in [1, n], j \in [1, n], j > i\}, \quad (3)$$

where $\mathcal{M}(\mathbf{x}, \tilde{h})$ is our membership features for an input $\mathbf{x}$ based on encoder $\tilde{h}$, and $S(\cdot, \cdot)$ measures the similarity between two feature vectors (e.g., $S(\cdot, \cdot)$ can be cosine similarity). Note that we omit the explicit dependency of $\mathcal{M}(\mathbf{x}, \tilde{h})$ on S, $\mathcal{A}$, and n for simplicity. There are $n \cdot (n-1)/2$ similarity scores in $\mathcal{M}(\mathbf{x}, \tilde{h})$ and they tend to be large if the input $\mathbf{x}$ is a member of the shadow encoder $\tilde{h}$.

Constructing an inference training dataset: Given the shadow member dataset $\mathcal{D}_s^m$, the shadow non-member dataset $\mathcal{D}_s^{nm}$, and the shadow encoder $\tilde{h}$, we construct an inference training dataset, which is used to build an inference classifier. In particular, given an input $\mathbf{x} \in \mathcal{D}_s^m$, we extract its membership features $\mathcal{M}(\mathbf{x}, \tilde{h})$ and assign a label 1 to it; and given an input $\mathbf{x} \in \mathcal{D}_s^{nm}$, we extract its membership features $\mathcal{M}(\mathbf{x}, \tilde{h})$ and assign a label 0 to it, where the label 1 represents "member" and the label 0 represents "non-member". Formally, our inference training dataset (denoted as $\mathcal{E}$) is as follows:

$$\mathcal{E} = \{(\mathcal{M}(\mathbf{x}, \tilde{h}), 1)|\mathbf{x} \in \mathcal{D}_s^m\} \cup \{(\mathcal{M}(\mathbf{x}, \tilde{h}), 0)|\mathbf{x} \in \mathcal{D}_s^{nm}\}. \quad (4)$$

Building inference classifiers: Given the inference training dataset $\mathcal{E}$, we build a binary inference classifier. We consider three types of classifiers, i.e., *vector-based classifier*, *set-based classifier*, and *threshold-based classifier*. These classifiers use the membership features differently. Next, we discuss them one by one.

- **Vector-based classifier (EncoderMI-V).** In a vector-based classifier, we transform the set of membership features $\mathcal{M}(\mathbf{x}, \tilde{h})$ of an input into a vector. Specifically, we rank the $n \cdot (n-1)/2$ similarity scores in $\mathcal{M}(\mathbf{x}, \tilde{h})$ in a descending order. We apply the ranking operation to the membership features of each input in the inference training dataset $\mathcal{E}$. Then, we train a vector-based classifier (e.g., a fully connected neural network) on $\mathcal{E}$ following the standard supervised learning procedure. We use f_v to denote the vector-based classifier. Moreover, we use *EncoderMI-V* to denote this method.
- **Set-based classifier (EncoderMI-S).** In a set-based classifier, we directly operate on the set of membership features $\mathcal{M}(\mathbf{x}, \tilde{h})$ of an input. In particular, we train a set-based classifier (e.g., DeepSets [53]) based on $\mathcal{E}$. A set-based classifier takes a *set* (i.e., $\mathcal{M}(\mathbf{x}, \tilde{h})$) as input and predicts a label (1 or 0) for it. A set-based classifier needs to be input-set-permutation-invariant, i.e., the predicted label does not rely on the order of the set elements. As a result, set-based classifiers and vector-based classifiers require substantially different neural network architectures. Moreover, set-based classification is generally harder than vector-based classification. For simplicity, we use f_s to denote the set-based classifier and we use *EncoderMI-S* to denote this method.
- **Threshold-based classifier (EncoderMI-T).** In a threshold-based classifier, we use the average similarity score in $\mathcal{M}(\mathbf{x}, \tilde{h})$ of an input to infer its membership. In particular, our threshold-based classifier predicts an input to be a member if and only if the average similarity score in its membership features $\mathcal{M}(\mathbf{x}, \tilde{h})$ is no smaller than a threshold. The key challenge is to

Algorithm 1 Our Membership Inference Method EncoderMI

```
Require: $f_v$ (or $f_s$ or $f_t$), $h$, $\mathcal{A}$, $n$, $S$, and $\mathbf{x}$
Ensure: Member or non-member
{$\mathbf{x}^1, \mathbf{x}^2, \cdots, \mathbf{x}^n$} $\leftarrow$ Augmentation($\mathbf{x}, \mathcal{A}, n$)
$\mathcal{M}(\mathbf{x}, h) \leftarrow \{S(h(\mathbf{x}^i), h(\mathbf{x}^j)) | i \in [1, n], j \in [1, n], j > i\}$
if $f_v$ then
    return $f_v$(Ranking($\mathcal{M}(\mathbf{x}, h)$))
else if $f_s$ then
    return $f_s(\mathcal{M}(\mathbf{x}, h))$
else if $f_t$ then
    return $f_t$(Average($\mathcal{M}(\mathbf{x}, h)$))
end if
```

determine the threshold with which the threshold-based classifier achieves high accuracy at membership inference. Given a threshold θ, we use $\alpha(\theta)$ (or $\beta(\theta)$) to denote the number of inputs in the shadow member (or non-member) dataset whose average similarity score in $\mathcal{M}(\mathbf{x}, \tilde{h})$ is smaller (or no smaller) than θ. The accuracy of our threshold-based classifier with the threshold θ for the shadow dataset is $1 - (\alpha(\theta) + \beta(\theta))/|\mathcal{D}_s|$. Our threshold-based classifier uses the optimal threshold θ^* that maximizes such accuracy, i.e., minimizes $\alpha(\theta) + \beta(\theta)$. If we plot the probability distribution of the average similarity score for shadow members and shadow non-members as two curves, where the x-axis is average similarity score and y-axis is the probability that a random shadow member (or non-member) has the average similarity score, then the threshold θ^* is the intersection point of the two curves.

Yeom et al. [52] and Song et al. [48] leveraged a similar threshold-based strategy for membership inference. Different from us, their methods were designed for classifiers and were based on the confidence scores outputted by a classifier.

4.3 Inferring Membership

Given a black-box access to the target encoder h and an input $\mathbf{x}$, we use the inference classifier f_v (or f_s or f_t) to predict whether the input $\mathbf{x}$ is a member of the target encoder h. Algorithm 1 shows our method . Given the input $\mathbf{x}$, the data augmentation module $\mathcal{A}$, and an integer n, the function Augmentation produces n augmented inputs. We use the target encoder h to produce a feature vector for each augmented input, and then we compute the set of pairwise similarity scores as the membership features $\mathcal{M}(\mathbf{x}, h)$ for the input $\mathbf{x}$. Finally, we use the inference classifier to infer the membership status of the input $\mathbf{x}$ based on the extracted membership features. The function Ranking ranks the similarity scores in $\mathcal{M}(\mathbf{x}, h)$ in a descending order, while the function Average computes the average of the similarity scores in $\mathcal{M}(\mathbf{x}, h)$.

5 EVALUATION

We evaluate EncoderMI on image encoders pre-trained on unlabeled images in this section. In Section 6, we apply EncoderMI to CLIP, which was pre-trained on unlabeled (image, text) pairs.

5.1 Experimental Setup

Datasets: We conduct our experiments on CIFAR10, STL10, and Tiny-ImageNet datasets.

- **CIFAR10 [30].** CIFAR10 dataset contains 60,000 colour images from 10 object categories. In particular, the dataset contains 50,000 training images and 10,000 testing images. The size of each image is 32 × 32.
- **STL10 [12].** STL10 dataset contains 13,000 labeled colour images from 10 classes. Specifically, the dataset is divided into 5,000 training images and 8,000 testing images. We note that STL10 dataset also contains 100,000 unlabeled images. The size of each image is 96 × 96 in this dataset.
- **Tiny-ImageNet [4].** Tiny-ImageNet dataset contains 100,000 training images and 10,000 testing images from 200 classes. Each class has 500 training images and 50 testing images. Each image has size 64 × 64.

Training target encoders: For CIFAR10 or Tiny-ImageNet, we randomly sample 10,000 images from its training data as the pre-training dataset to train a target encoder; and for STL10, we randomly sample 10,000 images from its unlabeled data as the pre-training dataset. By default, we use ResNet18 [21] as the architecture for the target encoder. Moreover, we use MoCo [20] to pre-train the target encoder on a pre-training dataset. We adopt the publicly available implementation of MoCo v1 [5] with the default parameter setting when pre-training our target encoders. Unless otherwise mentioned, we train a target encoder for 1,600 epochs. For CIFAR10 or Tiny-ImageNet, we treat its 10,000 testing images as ground truth "non-member" of the target encoder. For STL-10, we treat its 5,000 training images and the first 5,000 testing images as "non-member" of the target encoder. Therefore, unless otherwise mentioned, for each target encoder, we have 10,000 ground truth members and 10,000 ground truth non-members.

Training shadow encoders: In the scenario where the inferrer knows the pre-training data distribution of the target encoder, we randomly sample 20,000 images from the training or unlabeled data of the corresponding dataset as the shadow dataset. In the scenario where the inferrer does not know the pre-training data distribution, we randomly sample 20,000 images from the training data of CIFAR10 as the shadow dataset when the pre-training dataset is from STL-10, and we randomly sample 20,000 images from the unlabeled data of STL-10 as the shadow dataset when the pre-training dataset is CIFAR10 or Tiny-ImageNet.

We randomly split a shadow dataset into two disjoint sets, i.e., *shadow member dataset* and *shadow non-member dataset*, each of which contains 10,000 images. We train a shadow encoder using a shadow member dataset. We adopt the same architecture (i.e., ResNet18) for a shadow encoder if the inferrer knows the architecture of the target encoder and use VGG-11 [45] with batch normalization otherwise. We adopt the same training algorithm (i.e., MoCo) to pre-train a shadow encoder if the inferrer knows the algorithm used to pre-train the target encoder and adopt SimCLR [10] otherwise. We use the publicly available implementations [5, 6] with the default parameter settings for both training algorithms in our experiments. We train each shadow encoder for 1,600 epochs.

Building inference classifiers: We build inference classifiers based on a shadow dataset and a shadow encoder. EncoderMI-V uses a vector-based inference classifier. We use a fully connected neural network with two hidden layers as our vector-based classifier. In particular, the number of neurons in both hidden layers are 256. EncoderMI-S uses a set-based inference classifier. We choose DeepSets [53] as our set-based inference classifier. Moreover, we adopt the publicly available code for DeepSets [2] in our implementation. For both the vector-based classifier and the set-based classifier, we adopt cross-entropy as loss function and use Adam optimizer with initial learning rate of 0.0001 to train for 300 epochs. Note that EncoderMI-T leverages a threshold-based classifier and does not require training.

Evaluation metrics: Following previous work [42, 44], we adopt *accuracy*, *precision*, and *recall* to evaluate membership inference methods. Given an evaluation dataset that contains ground truth members and non-members of the target encoder, accuracy of a method is the ratio of the ground truth members/non-members that are correctly predicted by the method; precision of a method is the fraction of its predicted members that are indeed members; and recall of a method is the fraction of ground truth members that are predicted as members by the method.

Compared methods: Existing membership inference methods [11, 42, 44, 46, 48] aim to infer members of a classifier or a text embedding model. We generalize these methods to the contrastive learning setting as baseline methods. In particular, we compare our methods with the following five baseline methods, where the first three are for downstream classifiers, while the last two are for encoders.

Baseline-A. The target encoder is used to train a downstream classifier for a downstream task. Therefore, in this baseline method, we use the target encoder to train a downstream classifier (called *target downstream classifier*) for a downstream task, and then we apply existing membership inference methods [42, 44] to the target downstream classifier. In particular, we consider CIFAR10 as a downstream task and we randomly sample 10,000 of its training examples as the downstream dataset. The downstream dataset does not have overlap with the pre-training dataset and the shadow dataset. Given a shadow encoder and the downstream dataset, we train a downstream classifier (called *shadow downstream classifier*) via using the shadow encoder as a feature extractor. We query the confidence score vector for each input in the shadow member (or non-member) dataset outputted by the shadow downstream classifier and label it as "member" (or "non-member"). Given these confidence score vectors as well as the corresponding labels, we train a vector-based inference classifier. For a given input, we first query its confidence score vector outputted by the target downstream classifier and then use the inference classifier to predict whether it's a member of the target encoder. Note that, following previous work [42], we rank the confidence scores for an input, which outperforms unranked confidence scores.

Baseline-B. Choquette-Choo et al. [11] proposed label-only membership inference to a classifier. Roughly speaking, they construct a binary feature vector for an input based on some augmented versions of the input. An entry of the feature vector is 1 if and only if the corresponding augmented version is predicted correctly by the target classifier. This label-only membership inference method requires the ground truth label of an input. The pre-training data are unlabeled in contrastive learning, making the method not applicable to infer members of an encoder in practice. However, since the pre-training data CIFAR10 and Tiny-ImageNet have ground truth labels in our experiments, we assume an inferrer knows them and we evaluate the label-only method. Note that we cannot evaluate this method when the pre-training dataset is from STL10 as they are unlabeled. Similar to Baseline-A, we also apply this method to a target downstream classifier to infer members of the target encoder. For each input $\mathbf{x}$ in the shadow dataset, we create e augmented inputs. Moreover, we use the shadow downstream classifier to predict the label of $\mathbf{x}$ and each augmented input. We construct a binary vector $(b_0, b_1, b_2, \cdots, b_e)$ as the membership features for $\mathbf{x}$, where $b_0 = 1$ (or $b_i = 1$) if and only if the shadow downstream classifier correctly predicts the label of $\mathbf{x}$ (or the ith augmented input), where $i = 1, 2, \cdots, e$. We label the membership features of an input as "member" (or "non-member") if the input is in the shadow member (or non-member) dataset. Given membership features and their labels, we train a vector-based inference classifier. Then, we use the inference classifier to infer members of a target encoder via a target downstream classifier. We set $e = 10$ in our experiments.

Baseline-C. Song et al. [48] developed adversarial example based membership inference methods against classifiers. Specifically, they leverage the confidence scores produced by the target classifier for adversarial examples crafted from an input to infer whether the input is in the training dataset of the target classifier. For instance, their targeted adversarial example based method (discussed in Section 3.3.1 of [48]) first crafts $k - 1$ targeted adversarial examples for an input (one targeted adversarial example for each label that is not the input's ground truth label), then uses the target classifier to compute confidence scores for each of them, and finally concatenates the confidence scores as membership features for the input, where k is the number of classes in the target classifier. They train an inference classifier for each class of the target classifier and use the inference classifier corresponding to the ground truth label of an input to infer its membership.

Adversarial example of an input can be viewed as the input's augmented version. Therefore, we consider these methods in our experiments. We note that these methods require the ground truth label of an input and the ground truth label is one class of the downstream classifier. However, in contrastive learning, pre-training data often do not have labels. Moreover, even if the pre-training data have labels, their labels may not be the same as those of the downstream classifier. Therefore, we adapt the targeted adversarial example based method to a downstream classifier in our setting. Specifically, given an input $\mathbf{x}$, we use PGD [33] to generate k targeted adversarial examples based on a shadow downstream classifier, where k is the number of classes of the shadow downstream classifier. We then obtain k confidence score vectors outputted by the shadow downstream classifier for the k targeted adversarial examples, and we concatenate them as membership features for $\mathbf{x}$. Finally, we train one vector-based inference classifier based on the membership features of inputs in the shadow dataset, and we apply it to infer members of the target encoder via the target downstream classifier. Moreover, following [48], we set the perturbation budget (i.e., ϵ) to be $8/255$ when generating targeted adversarial examples.

Table 1: Accuracy, precision, and recall (%) of the five baseline methods. "–" means not applicable.

(a) Baseline-A

Pre-training dataset	Accuracy	Precision	Recall
CIFAR10	55.1	53.4	73.1
STL10	54.3	53.7	62.2
Tiny-ImageNet	47.3	48.2	68.3

(b) Baseline-B

Pre-training dataset	Accuracy	Precision	Recall
CIFAR10	54.6	63.1	58.2
STL10	–	–	–
Tiny-ImageNet	51.8	53.7	47.6

(c) Baseline-C

Pre-training dataset	Accuracy	Precision	Recall
CIFAR10	52.8	54.1	43.1
STL10	50.5	50.1	57.9
Tiny-ImageNet	50.2	52.1	42.3

(d) Baseline-D

Pre-training dataset	Accuracy	Precision	Recall
CIFAR10	50.7	50.6	51.0
STL10	50.1	49.9	50.3
Tiny-ImageNet	49.5	49.3	49.2

(e) Baseline-E

Pre-training dataset	Accuracy	Precision	Recall
CIFAR10	64.5	63.8	67.2
STL10	67.0	65.7	71.3
Tiny-ImageNet	68.6	67.8	70.8

Baseline-D. In this baseline method, we consider that an inferrer treats the target encoder as if it was a classifier. In other words, the inferrer treats the feature vector outputted by the target encoder for an input as if it was a *confidence score vector* outputted by a classifier. Therefore, we can apply the confidence score vector based methods [42, 44] to infer members of the target encoder. Specifically, given a shadow encoder, we use it to output a feature vector for each input in the corresponding shadow dataset. Moreover, we assign label "member" (or "non-member") to the feature vector of an input in the shadow member (or non-member) dataset. Then, we train a vector-based inference classifier using the feature vectors and their labels. Given a target encoder and an input, we first obtain the feature vector produced by the target encoder for the input. Then, based on the feature vector, the inference classifier predicts the input to be a member or non-member of the target encoder.

Baseline-E. Song et al. [46] studied membership inference to embedding models in the text domain. Their method can be used to infer whether a sentence is in the training dataset of a text embedding model. In particular, they use the average cosine similarity between the embedding vectors of the center word and each remaining word in a sentence to infer the membership of the sentence. We extend this method to our setting. Specifically, we could view an image as a "sentence" and each patch of an image as a "word". Then, we can use an image encoder to produce a feature vector for each patch. We view the center patch as the center word and compute its cosine similarity with each remaining patch. Finally, we use the average similarity score to infer the membership of the original image. Specifically, the image is predicted as a member if the average similarity score is larger than a threshold. Similar to our EncoderMI-T, we use a shadow dataset to determine the optimal threshold, i.e., we use the threshold that achieves the largest inference accuracy on the shadow dataset. We evenly divide an image into 3 × 1 (i.e., 3), 3 × 3 (i.e., 9), or 3 × 5 (i.e., 15) disjoint patches in our experiments. We found 3 × 3 achieves the best performance, so we will show results for 3 × 3 in the main text and defer the results for 3 × 1 and 3 × 5 to Appendix.

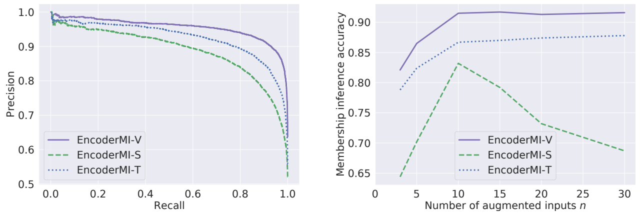

(a) **(b)**

Figure 1: (a) Precision-recall trade-off. (b) Impact of n on accuracy. The dataset is CIFAR10.

Parameter settings: We adopt the following default parameters for our method: we set $n = 10$ and we adopt cosine similarity as our similarity metric S since all contrastive learning algorithms use cosine similarity to measure similarity between two feature vectors. By default, we assume the inferrer knows the pre-training data distribution, the encoder architecture, and the training algorithm of the target encoder. Unless otherwise mentioned, we show results on CIFAR10 as the pre-training dataset. When the inferrer does not know the target encoder's training algorithm, we assume the inferrer uses random resized crop only to obtain augmented versions of an input when querying the target encoder because we found such data augmentation achieves the best performance. Note that we resize each image in STL10 and Tiny-ImageNet to 32 × 32 to be consistent with CIFAR10.

5.2 Experimental Results

Existing membership inference methods are insufficient: Table 1 shows the accuracy, precision, and recall of the five baseline methods. Note that we consider an inferrer with the strongest background knowledge in our threat model, i.e., the inferrer knows the pre-training data distribution, the encoder architecture, and the training algorithm. In other words, the shadow encoders are trained in the background knowledge $\mathcal{B} = (\surd, \surd, \surd)$. We find that the accuracies of Baseline-A, Baseline-B, Baseline-C, and Baseline-D are close to 50%, i.e., their accuracies are close to that of random guessing in which an input is predicted as a member or non-member with probability 0.5. The reason is that they were designed to infer members of a classifier instead of an encoder. The confidence score vector can capture whether the classifier is overfitted for the input, while the feature vector itself does not capture whether the encoder is overfitted for the input. As a result, these membership inference methods can infer the members of a classifier but not an encoder. Baseline-E is better than random guessing. The reason is that a

Table 2: Average accuracy, precision, and recall (%) of our methods for the target encoder pre-trained on CIFAR10 dataset. √ (or ×) means the inferrer has (or does not have) access to the corresponding background knowledge of the target encoder. The numbers in parenthesis are standard deviations in 5 trials.

Pre-training data distribution	Encoder architecture	Training algorithm	Accuracy			Precision			Recall		
			EncoderMI-V	EncoderMI-S	EncoderMI-T	EncoderMI-V	EncoderMI-S	EncoderMI-T	EncoderMI-V	EncoderMI-S	EncoderMI-T
×	×	×	86.2 (2.04)	78.1 (2.21)	82.1 (1.91)	87.8 (1.15)	78.9 (1.69)	80.1 (1.01)	89.3 (2.15)	86.8 (2.44)	87.2 (1.89)
√	×	×	86.9 (2.03)	79.6 (2.05)	83.3 (1.75)	88.3 (1.64)	79.8 (1.34)	81.0 (1.12)	90.9 (2.44)	87.4 (2.51)	89.2 (1.63)
×	√	×	87.0 (1.21)	79.4 (1.39)	83.5 (1.03)	88.4 (1.37)	79.6 (0.98)	81.6 (0.87)	91.4 (1.17)	87.2 (1.46)	87.9 (0.92)
×	×	√	86.7 (0.81)	79.2 (1.05)	83.0 (0.77)	88.2 (0.83)	79.9 (1.10)	80.4 (0.81)	91.4 (0.76)	87.1 (1.01)	89.1 (0.79)
√	√	×	87.2 (2.17)	79.9 (1.88)	83.6 (1.66)	88.4 (1.38)	80.1 (1.03)	81.9 (0.98)	91.5 (1.23)	87.9 (1.32)	87.9 (1.01)
√	×	√	87.6 (0.45)	80.3 (0.47)	84.2 (0.39)	88.7 (0.43)	80.6 (0.44)	83.1 (0.37)	91.7 (0.51)	87.7 (0.49)	88.0 (0.46)
×	√	√	90.2 (0.37)	81.1 (0.43)	85.2 (0.37)	89.5 (0.31)	80.5 (0.39)	85.1 (0.33)	93.3 (0.32)	88.2 (0.48)	88.9 (0.38)
√	√	√	91.4 (0.28)	83.1 (0.27)	86.6 (0.28)	90.1 (0.23)	80.8 (0.29)	85.9 (0.27)	93.5 (0.22)	88.3 (0.30)	89.1 (0.25)

patch of an input can be viewed as an augmented version of the input, and the similarity scores between patches capture the overfitting of an image encoder to some extent. However, the accuracy of Baseline-E is still low, compared to our EncoderMI.

Our methods are effective: Table 2, 5 (in Appendix), and 6 (in Appendix) show the accuracy, precision, and recall of our methods under the 8 different types of background knowledge for CIFAR10, STL-10, and Tiny-ImageNet datasets, respectively. The results are averaged in five trials. First, our methods are effective under all the 8 different types of background knowledge. For instance, our EncoderMI-V can achieve 88.7% – 96.5% accuracy on Tiny-ImageNet under the 8 types of background knowledge. Second, we find that EncoderMI-V is more effective than EncoderMI-S and EncoderMI-T in most cases. In particular, EncoderMI-V achieves higher accuracy (or precision or recall) than EncoderMI-S and EncoderMI-T in most cases. We suspect that EncoderMI-V outperforms EncoderMI-S because set-based classification is generally more challenging than vector-based classification, and thus viewing membership inference as a vector-based classification problem can achieve better inference performance. Our EncoderMI-T can achieve similar accuracy, precision, and recall with EncoderMI-S, which means that the average pairwise cosine similarity score for an input image already provides rich information about the input's membership status. Third, our methods achieve higher recall than precision, i.e., our methods predict more inputs as members than non-members. Fourth, the standard deviations tend to be larger when the inferrer has less background knowledge. This is because membership inference is less stable with less background knowledge.

Figure 1a shows the precision-recall trade-off of our three methods under the background knowledge $\mathcal{B} = (\surd, \surd, \surd)$. The curves are obtained via tuning the classification thresholds in the three inference classifiers to produce different precisions and recalls. Our results show that precision drops slightly as recall increases up to around 0.9, and then drops sharply as recall further increases.

Impact of the inferrer's background knowledge: Based on Table 2, 5, and 6, we have three major observations about the impact of the inferrer's background knowledge on our methods. First, EncoderMI-V achieves higher accuracy as the inferrer has access to more background knowledge, and we have the same observation for EncoderMI-S and EncoderMI-T in most cases. For instance, EncoderMI-V achieves 96.5% accuracy when the inferrer knows all the three dimensions of background knowledge while achieving 88.7% accuracy when the inferrer does not know any of them for Tiny-ImageNet dataset. Second, among the three dimensions of background knowledge, training algorithm is the most informative for STL10 and Tiny-ImageNet, while the three dimensions contribute equally for CIFAR10. For instance, on Tiny-ImageNet, EncoderMI-V achieves 94.1% accuracy when the inferrer only has access to the training algorithm, while EncoderMI-V respectively achieves 89.1% and 93.0% accuracy when the inferrer only has access to the encoder architecture and the pre-training data distribution. For CIFAR10, EncoderMI-V achieves around 86.8% accuracy when the inferrer only has access to any of the three dimensions. Third, there is no clear winner among the encoder architecture and pre-training data distribution. For instance, having access to the pre-training data distribution alone (i.e., $\mathcal{B} = (\surd, \times, \times)$) achieves higher accuracy than having access to the encoder architecture alone (i.e., $\mathcal{B} = (\times, \surd, \times)$) for all our three methods on Tiny-ImageNet, but we observe the opposite for EncoderMI-V and EncoderMI-T on STL10.

Table 3: Accuracy, precision, and recall (%) of our methods with different similarity metrics. The dataset is CIFAR10.

Method	Similarity metric	Accuracy	Precision	Recall
EncoderMI-V	Cosine	91.5	90.0	93.5
	Correlation	89.3	87.9	92.2
	Euclidean	88.9	85.3	94.5
EncoderMI-S	Cosine	83.2	80.5	87.9
	Correlation	76.3	75.5	78.5
	Euclidean	75.8	73.6	81.4
EncoderMI-T	Cosine	86.7	85.7	89.0
	Correlation	80.6	79.8	81.6
	Euclidean	80.7	80.1	82.5

Impact of n: Figure 1b shows the impact of the number of augmented inputs n on the accuracy of our methods for CIFAR10, where the inferrer's background knowledge is $\mathcal{B} = (\surd, \surd, \surd)$. We observe that, for EncoderMI-V and EncoderMI-T, the accuracy first increases and then saturates as n increases. However, for EncoderMI-S, the accuracy first increases and then decreases as n increases. We suspect the reason is that as n increases, the number of pairwise similarity scores in the membership features increases exponentially, making set-based classification harder.

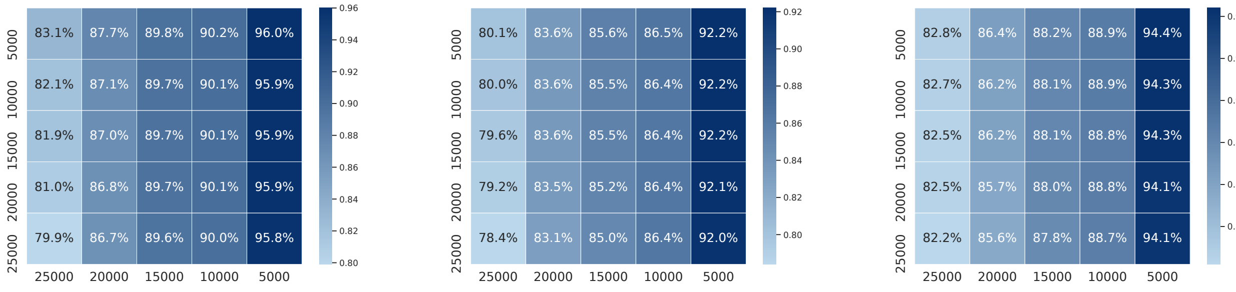

(a) EncoderMI-V

(b) EncoderMI-S

(c) EncoderMI-T

Figure 2: Impact of the size of the pre-training dataset (x-axis) and the shadow dataset (y-axis) on the accuracy of membership inference. Both the pre-training dataset and shadow dataset are randomly sampled from STL10.

Impact of the similarity metric S: Table 3 shows the impact of the similarity metric S on our methods, where "Correlation" refers to Pearson correlation coefficient. We have two observations from the experimental results. First, the cosine similarity metric achieves the highest accuracy (or precision or recall). The reason is that the cosine similarity metric is also used in the pre-training of the target encoder. Second, our methods still achieve high accuracy (or precision or recall) when using different similarity metrics from the one used in the pre-training of the target encoder.

Impact of the size of the pre-training and shadow datasets: Figure 2 shows the impact of the size of the pre-training dataset and the shadow dataset on the accuracy of our three methods, where the inferrer's background knowledge is $\mathcal{B} = (\surd, \surd, \surd)$. Both the pre-training dataset and shadow dataset are randomly sampled from the unlabeled data of STL10, but they do not have overlaps. Note that we did not use CIFAR10 in these experiments because its dataset size is small and we cannot sample disjoint pre-training and shadow datasets with large sizes. First, we observe that the accuracy of our methods increases as the pre-training dataset becomes smaller. The reason is that the target encoder is more overfitted to the pre-training dataset when its size is smaller. Second, our methods are less sensitive to the shadow dataset size. In particular, given a pre-training dataset size, each of our three methods achieves similar accuracy when the shadow dataset size ranges between 5,000 and 25,000. Our results show that the shadow encoder pre-trained on shadow dataset with various sizes can mimic the behavior of the target encoder in terms of membership inference.

Impact of data augmentation: The data augmentation operations an inferrer uses may be different from those used to pre-train the target encoder. In this experiment, we explicitly study the impact of data augmentation. We assume the inferrer uses a comprehensive list of four commonly used data augmentation operations, i.e., random grayscale, random resized crop, random horizontal flip, and color jitter. We gradually increase the number of overlapped data augmentation operations between the inferrer's comprehensive list and the target encoder. In particular, the target encoder starts from only using data augmentation operation Gaussian blur, which is not in the inferrer's list. Then, we add the inferrer's data augmentation operations to the target encoder's pre-training module one by one in the following order: random grayscale, random resized crop, random horizontal flip, and color jitter. We calculate the membership inference accuracy and the classification accuracy of the downstream classifier for each target encoder, where the downstream classifier is built as in Baseline-A. Figure 3 shows the results. We observe the number of overlapped data augmentation operations between the referrer and the target encoder controls a trade-off between membership inference accuracy and utility of the target encoder, i.e., the target encoder is more resistant against membership inference but the downstream classifier is also less accurate when the target encoder uses less data augmentation operations from the referrer's comprehensive list.

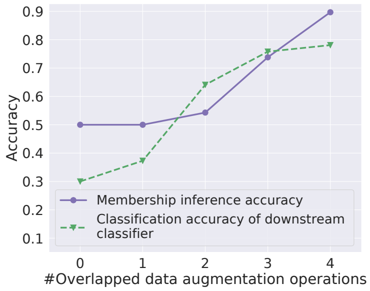

Figure 3: Impact of data augmentation, where the method is EncoderMI-V and the dataset is CIFAR10.

6 APPLYING OUR METHOD TO CLIP

CLIP [38] jointly pre-trains an image encoder and a text encoder on 400 million (image, text) pairs collected from the Internet. OpenAI has made the image encoder and text encoder publicly available. We view CLIP's image encoder with the ViT-B/32 architecture as the target encoder and apply our EncoderMI to infer its members. Specifically, given an input image, we aim to use EncoderMI to infer whether it was used by CLIP or not. Next, we first introduce experimental setup and then present experimental results.

6.1 Experimental Setup

Potential members and ground truth non-members: To evaluate our EncoderMI for CLIP's image encoder, we need an evaluation dataset consisting of both ground truth members and non-members. However, the pre-training dataset of CLIP is not released to the public. Therefore, we cannot obtain ground truth members of CLIP.

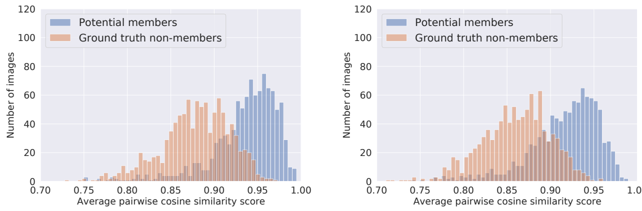

(a) Google **(b) Flickr**

Figure 4: Histograms of the average pairwise cosine similarity for potential members and ground truth non-members.

However, we can collect some images that are *potential members* and *ground truth non-members* of the CLIP's pre-training dataset. Specifically, according to Radford et al. [38], the (image, text) pairs used to pre-train CLIP were collected from the Internet based on a set of 500,000 popular keywords. Therefore, we collect the following two evaluation datasets, each of which has 1,000 potential members and 1,000 ground truth non-members:

- **Google.** We use the class names of CIFAR100 [30] as keywords and use Google image search to collect images. Appendix A shows the complete list of class names, e.g., "clock", "house", and "bus". In particular, we use a publicly available tool[1] to crawl images from Google search based on the keywords. We collected 10 images for each keyword, and thus we collected 1,000 images in total. We treat these images as *potential members* as they were potentially also collected and used by CLIP. To construct ground truth non-members, we further collected 2,000 images from Google search using the keywords. We randomly divided them into 1,000 pairs; and for each pair, we resized the two images to the same size, and we concatenated them to form a new image, which results in 1,000 images in total. We treat these images as ground truth non-members of CLIP.
- **Flickr.** Similar to the above Google evaluation dataset, we collected an evaluation dataset from Flickr using the 100 keywords and a publicly available tool[2]. Specifically, we collected 1,000 images as potential members. Moreover, we further collected 2,000 images and randomly paired them to be 1,000 images, which we treat as ground truth non-members.

We acknowledge that some of the potential members may not be ground truth members of CLIP in both of our evaluation datasets. For each potential member and ground truth non-member, we resize them as the input size of CLIP, which is 224 × 224.

Inference classifiers: We assume the inferrer does not know the pre-training data distribution, encoder architecture, and training algorithm of CLIP, which is the most difficult scenario for our EncoderMI. We use the inference classifiers we built in our previous experiments in Section 5. Specifically, in our previous experiments, for each of our three methods (i.e., EncoderMI-V, EncoderMI-S, and EncoderMI-T) and each of the three shadow datasets (i.e., CIFAR10, STL10, and Tiny-ImageNet), we have built 8 inference classifiers corresponding to the 8 types of background knowledge. We use the inference classifiers corresponding to the background knowledge $\mathcal{B} = (\surd, \surd, \surd)$ in our previous experiments (i.e., the inference classifiers corresponding to the last rows of Table 2, Table 5, and Table 6) to infer members of CLIP. Given an input image, we create 10 augmented inputs and use the CLIP's image encoder to produce a feature vector for each of them. Then, we compute the 45 pairwise cosine similarity scores between the 10 feature vectors, which constitute the set of membership features for the input image. Our inference classifiers predict the membership status of the input image based on the membership features.

Table 4: Accuracy, precision, and recall (%) of EncoderMI for CLIP's image encoder.

(a) Google

Method	Shadow dataset	Accuracy	Precision	Recall
EncoderMI-V	CIFAR10	70.0	64.5	88.8
	STL10	71.0	65.4	88.9
	Tiny-ImageNet	67.6	62.0	90.7
EncoderMI-S	CIFAR10	74.7	70.2	87.1
	STL10	74.6	70.2	86.8
	Tiny-ImageNet	73.2	68.1	88.1
EncoderMI-T	CIFAR10	70.3	64.2	89.7
	STL10	71.5	65.6	90.0
	Tiny-ImageNet	66.3	62.4	90.1

(b) Flickr

Method	Shadow dataset	Accuracy	Precision	Recall
EncoderMI-V	CIFAR10	74.9	72.0	81.5
	STL10	73.5	70.9	79.3
	Tiny-ImageNet	74.7	73.1	78.2
EncoderMI-S	CIFAR10	71.7	69.1	79.2
	STL10	72.7	71.4	76.4
	Tiny-ImageNet	71.6	69.3	79.0
EncoderMI-T	CIFAR10	73.9	68.8	80.1
	STL10	74.5	70.8	80.8
	Tiny-ImageNet	74.3	71.2	79.4

6.2 Experimental Results

Cosine similarity score distribution for potential members and ground truth non-members: Recall that, for each potential member or ground truth non-member, EncoderMI constructs membership features consisting of 45 pairwise cosine similarity scores. We compute the average of the 45 pairwise cosine similarity scores for each potential member or ground truth non-member. Figure 4 shows the histograms of the average pairwise cosine similarity scores for potential members and ground truth non-members in our two evaluation datasets. We observe that the potential members and ground truth non-members are statistically distinguishable with respect to the average pairwise cosine similarity scores. In particular, the potential members tend to have larger average pairwise cosine similarity scores than the ground truth non-members.

Effectiveness of EncoderMI: Table 4 shows the accuracy, precision, and recall of the three variants of EncoderMI based on different shadow datasets when applied to the CLIP's image encoder. The accuracy, precision, and recall are calculated based on the 1,000 potential members and 1,000 ground truth non-members in each evaluation dataset. First, we observe that EncoderMI based on different shadow datasets achieves high accuracy, e.g., 0.66 – 0.75. Our results imply that overfitting exists in real-world image encoders

[1] https://github.com/hardikvasa/google-images-download
[2] https://stuvel.eu/software/flickrapi

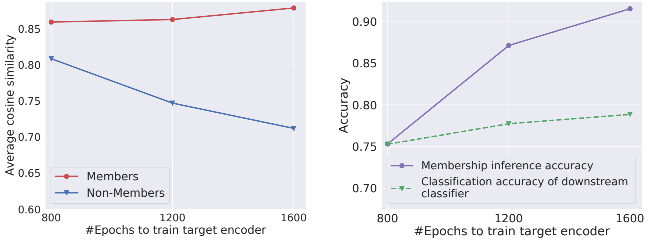

(a) Overfitting of the target encoder **(b) Inferability-utility tradeoff**

Figure 5: (a) The target encoder is more overfitted to its pre-training data when it's pre-trained for more epochs. (b) Trade-off between membership inference accuracy and encoder utility for early stopping, where the method is EncoderMI-V and the dataset is CIFAR10.

such as CLIP. Second, EncoderMI achieves a higher recall than precision, which means that EncoderMI predicts a large fraction of potential members as members. Third, our EncoderMI achieves higher recall (or lower precision) on Google than Flickr. In other words, our EncoderMI predicts more inputs from Google image search as members. The reason is that, on average, the average pairwise cosine similarity score for inputs from Google image search is larger than that for inputs from Flickr as shown in Figure 4.

7 DISCUSSION ON COUNTERMEASURES

Preventing overfitting via early stopping: Recall that our EncoderMI exploits the overfitting of a target encoder on its pre-training dataset. Note that the overfitting of a target encoder on its pre-training dataset is different from that of a classifier. For instance, when a classifier is overfitted to its training dataset, it may have different classification accuracies on its training dataset and testing dataset. Moreover, the confidence score vectors outputted by the classifier for its training dataset and testing dataset are also statistically distinguishable. Given an input, a target encoder outputs a feature vector for it. However, the feature vector itself does not capture the overfitting of the target encoder on the input. Instead, when the target encoder is overfitted to its pre-training dataset, it may output more similar feature vectors for the augmented versions of an input in the pre-training dataset.

We find that a target encoder is more overfitted to its pre-training dataset when it is trained for more epochs. Recall that the membership features for an input constructed by our EncoderMI consist of 45 pairwise cosine similarity scores. For each member or non-member of the target encoder, we compute the average pairwise cosine similarity scores in its membership features, and we further compute the average pairwise cosine similarity scores over all members (or non-members). Figure 5a shows the average pairwise cosine similarity scores for members and non-members of the target encoder as the number of pre-training epochs increases, where the pre-training dataset is based on CIFAR10. We observe the average pairwise cosine similarity increases (or decreases) for members (or non-members) as the number of epochs increases. In other words, the target encoder is more overfitted to its pre-training dataset when pre-training it for more epochs.

Our observation inspires us to counter EncoderMI via preventing overfitting through early stopping, i.e., pre-training a target encoder for less number of epochs. We evaluate the early stopping based countermeasure against our EncoderMI. In particular, we pre-train a target encoder on the pre-training dataset based on CIFAR10. After we pre-train the target encoder for some epochs, we calculate the accuracy of our EncoderMI-V under the background knowledge $\mathcal{B} = (\surd, \surd, \surd)$ and we also calculate the classification accuracy of a downstream classifier built based on the target encoder. Both the pre-training dataset and the downstream dataset are constructed based on CIFAR10 as we described in Section 5, and the classification accuracy of the downstream classifier is calculated based on the testing dataset of CIFAR10. Figure 5b shows the membership inference accuracy of our EncoderMI-V and the classification accuracy of the downstream classifier as we pre-train the target encoder for more epochs. We observe that the early stopping based defense achieves a trade-off, i.e., it decreases the membership inference accuracy but also reduces the classification accuracy of the downstream classifier. We note that Song et al. [47] found that early stopping outperforms other overfitting-prevention countermeasures against membership inference to classifiers, and they also observed a trade-off between membership inference accuracy and classifier utility for early stopping.

Pre-training with differential privacy: Differential privacy [7, 15, 26, 36, 43] can provide formal membership privacy guarantees for each input in the training dataset of a machine learning model. Many differentially private learning algorithms have been proposed. These algorithms add noise to the training data [14], the objective function [25, 26], or the gradient computed by (stochastic) gradient descent during the learning process [7, 26, 43]. For instance, Abadi et al. [7] proposed differentially private stochastic gradient descent (DP-SGD) which adds random Gaussian noise to the gradient computed by stochastic gradient descent. It would be interesting future work to generalize these differentially private learning algorithms to contrastive learning. In particular, when the pre-training dataset changes by one input, the encoder learnt by a differentially private contrastive learning algorithm does not change much. However, differential privacy may also incur large utility loss for the encoder, i.e., the downstream classifiers built based on a differentially private encoder may have much lower classification accuracy.

Adversarial learning: Adversarial learning based countermeasures [29, 34] have been studied to mitigate membership inference to classifiers, which were inspired by adversarial learning based countermeasures against attribute inference attacks [27]. For instance, Nasr et al. [34] proposed to add an adversarial regularization term to the loss function when training a target classifier, where the adversarial regularization term models a membership inference method's accuracy. Jia et al. [29] proposed MemGuard which does not modify the training process, but adds carefully crafted perturbation to the confidence score vector outputted by the target classifier for each input. Specifically, the idea is to turn the perturbed confidence score vector to be an adversarial example to the inference classifiers, which make random membership inference based on the perturbed confidence score vector. It would be interesting future work to extend these countermeasures to pre-trained encoders. For instance, we may capture our EncoderMI's accuracy as an adversarial regularization term and add it to the contrastive loss when pre-training an encoder using contrastive learning; we may also add carefully crafted perturbation to the feature vector outputted by an encoder for each (augmented) input such that the set of membership features constructed by our EncoderMI for an input becomes an adversarial example to the inference classifiers, which make random membership inference based on the perturbed membership features. A key challenge is how to find such perturbation to each feature vector since the membership features depend on the pairwise similarity between a set of feature vectors corresponding to the augmented versions of an input.

8 RELATED WORK

Membership inference: In membership inference against machine learning classifiers [11, 18, 19, 22, 24, 31, 32, 32, 35, 35, 41, 42, 44, 47, 48, 52], an inferrer aims to infer whether an input is in the training dataset of a classifier (called *target classifier*). For instance, in the methods proposed by Shokri et al. [44], an inferrer first trains shadow classifiers to mimic the behaviors of the target classifier. Given the shadow classifiers whose ground truth members and non-members are known to the inferrer, the inferrer trains inference classifiers, which are then applied to infer members of the target classifier. Salem et al. [42] further improved these methods by relaxing the assumptions about the inferrer. Hui et al. [24] proposed blind membership inference methods that do not require training shadow classifiers. Concurrent to our work, He et al. [22] also studied membership inference against contrastive learning. They assume the pre-training data and downstream data are the same. Specifically, given a labeled training dataset, they first use contrastive learning to pre-train an encoder and then use it to fine-tune a classifier on the labeled training dataset. They try to infer whether an input is in the labeled training dataset via applying existing methods [42, 44] to the fine-tuned classifier.

Our methods are different from these ones as they were designed to infer members of a *classifier* while our methods aim to infer members of an encoder pre-trained by contrastive learning. Our experimental results show that these methods achieve accuracy close to random guessing when applied to infer members of an encoder. The reason is that the confidence score vector outputted by a classifier can capture whether the classifier is overfitted for an input, while the feature vector itself outputted by an encoder does not capture whether the encoder is overfitted for an input. The similarity scores between the feature vectors of the augmented versions of an input capture whether the encoder is overfitted for the input, and our methods leverage such similarity scores to infer the membership status of the input.

Existing membership inference methods for pre-trained models [8, 46] focused on the natural language domain. For instance, Carlini et al. [8] proposed membership inference methods for GPT-2 [39], which is a pre-trained language model, and they further leveraged the membership inference methods to reconstruct the training data of GPT-2. Specifically, they first reconstructed some candidate texts and then applied a membership inference method to determine the membership status of each candidate text. To the best of our knowledge, no prior work has studied membership inference for encoders in the image domain.

Prior work [23, 54] also studied membership inference against transfer learning. For instance, Hidano et al. [23] assume a white-box access to the transferred part of the teacher model while Zou et al. [54] leverage the posterior of the teacher model. Our work is different from these, because pre-training an image encoder is different from training a teacher model since the former uses contrastive learning on unlabeled data while the latter uses the standard supervised learning on labeled data.

Countermeasures against membership inference: Many countermeasures [9, 29, 31, 34, 42, 44, 47] were proposed to counter membership inference for classifiers. The first category of countermeasures [42, 44, 47] try to prevent overfitting when training classifiers, e.g., standard L_2 regularization [44], dropout [42], and early stopping [47]. The second category of countermeasures [7, 43] are based on differential privacy [15], which often incur large utility loss for the learnt machine learning classifiers. The third category of countermeasures leverage adversarial learning, e.g., adversarial regularization [34] and MemGuard [29]. We explored an early stopping based countermeasure against our EncoderMI. Our results show that such countermeasure achieves a trade-off between membership inference accuracy and utility of an encoder.

Contrastive learning: Contrastive learning [10, 13, 17, 20, 37, 40, 50] aims to pre-train image encoders on unlabeled data via exploiting the supervisory signals in the unlabeled data itself. The unlabeled data could be unlabeled images or (image, text) pairs. The pre-trained encoders can be used for many downstream tasks. The key idea of contrastive learning is to pre-train an image encoder such that it outputs similar feature vectors for a pair of augmented inputs created from the same input image and outputs dissimilar feature vectors for a pair of augmented inputs created from different input images. Examples of contrastive learning methods include MoCo [20], SimCLR [10], and CLIP [38], which we discussed in Section 2. We note that Jia et al. [28] proposed BadEncoder, which embeds backdoors into a pre-trained image encoder such that multiple downstream classifiers built based on the backdoored encoder inherit the backdoor behavior simultaneously.

9 CONCLUSION AND FUTURE WORK

In this work, we propose the first membership inference method against image encoders pre-trained by contrastive learning. Our method exploits the overfitting of an image encoder, i.e., it produces more similar feature vectors for two augmented versions of the same input. Our experimental results on image encoders pre-trained on multiple datasets by ourselves as well as a real-world image encoder show that our method can achieve high accuracy, precision, and recall. Moreover, we also find that an early stopping based countermeasure achieves a trade-off between membership inference accuracy and encoder utility.

Interesting future work includes 1) extending our method to the white-box settings in which the inferrer has access to the parameters of the target encoder, 2) extending our method to infer the membership of an (image, text) pair, 3) developing new countermeasures against our method, and 4) exploring other privacy/confidentiality risks of pre-trained image encoders such as stealing their parameters [49] and hyperparameters (e.g., encoder architecture) [51].

Acknowledgements: We thank the anonymous reviewers and our shepherd Reza Shokri for constructive comments. This work was supported by NSF under Grant No. 1937786.

REFERENCES

[1] 2020. Twitter demands AI company stops 'collecting faces'. https://www.bbc.com/news/technology-51220654. (2020).

[2] 2021. DeepSets. https://github.com/manzilzaheer/DeepSets. (2021).

[3] 2021. FTC settlement with Ever orders data and AIs deleted after facial recognition pivot. https://techcrunch.com/2021/01/12/ftc-settlement-with-ever-orders-data-and-ais-deleted-after-facial-recognition-pivot. (2021).

[4] 2021. MicroImageNet classification challenge. https://www.kaggle.com/c/tiny-imagenet/overview. (2021).

[5] 2021. MoCo. https://github.com/facebookresearch/moco. (2021).

[6] 2021. SimCLR. https://github.com/leftthomas/SimCLR. (2021).

[7] Martin Abadi, Andy Chu, Ian Goodfellow, H Brendan McMahan, Ilya Mironov, Kunal Talwar, and Li Zhang. 2016. Deep learning with differential privacy. In *CCS*.

[8] Nicholas Carlini, Florian Tramer, Eric Wallace, Matthew Jagielski, Ariel Herbert-Voss, Katherine Lee, Adam Roberts, Tom Brown, Dawn Song, Ulfar Erlingsson, et al. 2021. Extracting Training Data from Large Language Models. In *USENIX Security Symposium*.

[9] Qingrong Chen, Chong Xiang, Minhui Xue, Bo Li, Nikita Borisov, Dali Kaarfar, and Haojin Zhu. 2018. Differentially private data generative models. *arXiv preprint arXiv:1812.02274* (2018).

[10] Ting Chen, Simon Kornblith, Mohammad Norouzi, and Geoffrey Hinton. 2020. A simple framework for contrastive learning of visual representations. In *ICML*.

[11] Christopher A Choquette Choo, Florian Tramer, Nicholas Carlini, and Nicolas Papernot. 2021. Label-only membership inference attacks. In *ICML*.

[12] Adam Coates, Andrew Ng, and Honglak Lee. 2011. An analysis of single-layer networks in unsupervised feature learning. In *AISTATS*.

[13] Alexey Dosovitskiy, Philipp Fischer, Jost Tobias Springenberg, Martin Riedmiller, and Thomas Brox. 2015. Discriminative unsupervised feature learning with exemplar convolutional neural networks. *IEEE transactions on pattern analysis and machine intelligence* 38, 9 (2015), 1734–1747.

[14] John C Duchi, Michael I Jordan, and Martin J Wainwright. 2013. Local privacy and statistical minimax rates. In *FOCS*.

[15] Cynthia Dwork, Frank McSherry, Kobbi Nissim, and Adam Smith. 2006. Calibrating noise to sensitivity in private data analysis. In *TCC*.

[16] Daryl LX Fung, Qian Liu, Judah Zammit, Carson Kai-Sang Leung, and Pingzhao Hu. 2021. Self-supervised deep learning model for COVID-19 lung CT image segmentation highlighting putative causal relationship among age, underlying disease and COVID-19. *Journal of Translational Medicine* 19, 1 (2021).

[17] Raia Hadsell, Sumit Chopra, and Yann LeCun. 2006. Dimensionality reduction by learning an invariant mapping. In *CVPR*.

[18] Inken Hagestedt, Mathias Humbert, Pascal Berrang, Irina Lehmann, Roland Eils, Michael Backes, and Yang Zhang. 2020. Membership inference against DNA methylation databases. In *EuroS&P*.

[19] Inken Hagestedt, Yang Zhang, Mathias Humbert, Pascal Berrang, Haixu Tang, XiaoFeng Wang, and Michael Backes. 2019. MBeacon: Privacy-Preserving Beacons for DNA Methylation Data. In *NDSS*.

[20] Kaiming He, Haoqi Fan, Yuxin Wu, Saining Xie, and Ross Girshick. 2020. Momentum contrast for unsupervised visual representation learning. In *CVPR*.

[21] Kaiming He, Xiangyu Zhang, Shaoqing Ren, and Jian Sun. 2016. Deep residual learning for image recognition. In *CVPR*.

[22] Xinlei He and Yang Zhang. 2021. Quantifying and Mitigating Privacy Risks of Contrastive Learning. *arXiv preprint arXiv:2102.04140* (2021).

[23] Seira Hidano, Takao Murakami, and Yusuke Kawamoto. 2021. TransMIA: Membership Inference Attacks Using Transfer Shadow Training. In *IJCNN*.

[24] Bo Hui, Yuchen Yang, Haolin Yuan, Philippe Burlina, Neil Zhenqiang Gong, and Yinzhi Cao. 2021. Practical Blind Membership Inference Attack via Differential Comparisons. In *NDSS*.

[25] Roger Iyengar, Joseph P Near, Dawn Song, Om Thakkar, Abhradeep Thakurta, and Lun Wang. 2019. Towards practical differentially private convex optimization. In *IEEE S & P*.

[26] Bargav Jayaraman and David Evans. 2019. Evaluating differentially private machine learning in practice. In *USENIX Security Symposium*.

[27] Jinyuan Jia and Neil Zhenqiang Gong. 2018. AttriGuard: A practical defense against attribute inference attacks via adversarial machine learning. In *USENIX Security Symposium*.

[28] Jinyuan Jia, Yupei Liu, and Neil Zhenqiang Gong. 2022. BadEncoder: Backdoor Attacks to Pre-trained Encoders in Self-Supervised Learning. In *IEEE S & P*.

[29] Jinyuan Jia, Ahmed Salem, Michael Backes, Yang Zhang, and Neil Zhenqiang Gong. 2019. Memguard: Defending against black-box membership inference attacks via adversarial examples. In *CCS*.

[30] Alex Krizhevsky. 2009. Learning multiple layers of features from tiny images. *Tech Report* (2009).

[31] Jiacheng Li, Ninghui Li, and Bruno Ribeiro. 2021. Membership Inference Attacks and Defenses in Classification Models. In *CODASPY*.

[32] Zheng Li and Yang Zhang. 2021. Membership Leakage in Label-Only Exposures. In *CCS*.

[33] Aleksander Madry, Aleksandar Makelov, Ludwig Schmidt, Dimitris Tsipras, and Adrian Vladu. 2018. Towards Deep Learning Models Resistant to Adversarial Attacks. In *ICLR*.

[34] Milad Nasr, Reza Shokri, and Amir Houmansadr. 2018. Machine learning with membership privacy using adversarial regularization. In *CCS*.

[35] Milad Nasr, Reza Shokri, and Amir Houmansadr. 2019. Comprehensive privacy analysis of deep learning: Passive and active white-box inference attacks against centralized and federated learning. In *IEEE S & P*.

[36] Milad Nasr, Shuang Song, Abhradeep Thakurta, Nicolas Papernot, and Nicholas Carlini. 2021. Adversary Instantiation: Lower Bounds for Differentially Private Machine Learning. In *IEEE S & P*.

[37] Aaron van den Oord, Yazhe Li, and Oriol Vinyals. 2018. Representation learning with contrastive predictive coding. *arXiv preprint arXiv:1807.03748* (2018).

[38] Alec Radford, Jong Wook Kim, Chris Hallacy, Aditya Ramesh, Gabriel Goh, Sandhini Agarwal, Girish Sastry, Amanda Askell, Pamela Mishkin, Jack Clark, et al. 2021. Learning transferable visual models from natural language supervision. *arXiv preprint arXiv:2103.00020* (2021).

[39] Alec Radford, Jeffrey Wu, Rewon Child, David Luan, Dario Amodei, and Ilya Sutskever. 2019. Language models are unsupervised multitask learners. *OpenAI blog* 1, 8 (2019), 9.

[40] Marc'Aurelio Ranzato, Fu Jie Huang, Y-Lan Boureau, and Yann LeCun. 2007. Unsupervised learning of invariant feature hierarchies with applications to object recognition. In *CVPR*.

[41] Alexandre Sablayrolles, Matthijs Douze, Cordelia Schmid, Yann Ollivier, and Hervé Jégou. 2019. White-box vs black-box: Bayes optimal strategies for membership inference. In *ICML*.

[42] Ahmed Salem, Yang Zhang, Mathias Humbert, Pascal Berrang, Mario Fritz, and Michael Backes. 2019. Ml-leaks: Model and data independent membership inference attacks and defenses on machine learning models. In *NDSS*.

[43] Reza Shokri and Vitaly Shmatikov. 2015. Privacy-preserving deep learning. In *CCS*.

[44] Reza Shokri, Marco Stronati, Congzheng Song, and Vitaly Shmatikov. 2017. Membership inference attacks against machine learning models. In *IEEE S & P*.

[45] Karen Simonyan and Andrew Zisserman. 2015. Very deep convolutional networks for large-scale image recognition. In *ICLR*.

[46] Congzheng Song and Ananth Raghunathan. 2020. Information leakage in embedding models. In *CCS*.

[47] Liwei Song and Prateek Mittal. 2021. Systematic evaluation of privacy risks of machine learning models. In *USENIX Security Symposium*.

[48] Liwei Song, Reza Shokri, and Prateek Mittal. 2019. Privacy risks of securing machine learning models against adversarial examples. In *CCS*.

[49] Florian Tramèr, Fan Zhang, Ari Juels, Michael K Reiter, and Thomas Ristenpart. 2016. Stealing machine learning models via prediction apis. In *USENIX Security Symposium*.

[50] Pascal Vincent, Hugo Larochelle, Yoshua Bengio, and Pierre-Antoine Manzagol. 2008. Extracting and composing robust features with denoising autoencoders. In *ICML*.

[51] Binghui Wang and Neil Zhenqiang Gong. 2018. Stealing hyperparameters in machine learning. In *IEEE S & P*.

[52] Samuel Yeom, Irene Giacomelli, Matt Fredrikson, and Somesh Jha. 2018. Privacy risk in machine learning: Analyzing the connection to overfitting. In *CSF*.

[53] Manzil Zaheer, Satwik Kottur, Siamak Ravanbakhsh, Barnabas Poczos, Ruslan Salakhutdinov, and Alexander Smola. 2017. Deep sets. In *NeurIPS*.

[54] Yang Zou, Zhikun Zhang, Michael Backes, and Yang Zhang. 2020. Privacy Analysis of Deep Learning in the Wild: Membership Inference Attacks against Transfer Learning. *arXiv preprint arXiv:2009.04872* (2020).

A KEYWORDS FOR GOOGLE SEARCH AND FLICKR CRALWER

The keywords are the 100 class names in CIFAR100: beaver, dolphin, otter, seal, whale, aquarium fish, flatfish, ray, shark, trout, orchids, poppies, roses, sunflowers, tulips, bottles, bowls, cans, cups, plates, apples, mushrooms, oranges, pears, sweet peppers, clock, computer keyboard, lamp, telephone, television, bed, chair, couch, table, wardrobe, bee, beetle, butterfly, caterpillar, cockroach, bear, leopard, lion, tiger, wolf, bridge, castle, house, road, skyscraper, cloud, forest, mountain, plain, sea, camel, cattle, chimpanzee, elephant, kangaroo, fox, porcupine, possum, raccoon, skunk, crab, lobster, snail, spider, worm, baby, boy, girl, man, woman, crocodile, dinosaur, lizard, snake, turtle, hamster, mouse, rabbit, shrew, squirrel, maple, oak,

Table 5: Average accuracy, precision, and recall (%) of our methods for the target encoder pre-trained on STL10 dataset. √ (or ×) means the inferrer has (or does not have) access to the corresponding background knowledge of the target encoder. The numbers in parenthesis are standard deviations in 5 trials.

Pre-training data distribution	Encoder architecture	Training algorithm	Accuracy			Precision			Recall		
			EncoderMI-V	EncoderMI-S	EncoderMI-T	EncoderMI-V	EncoderMI-S	EncoderMI-T	EncoderMI-V	EncoderMI-S	EncoderMI-T
×	×	×	81.9 (1.94)	80.4 (1.79)	81.3 (1.74)	79.1 (2.35)	77.2 (2.04)	78.4 (1.87)	90.2 (2.79)	92.0 (2.61)	90.3 (2.03)
√	×	×	83.8 (1.81)	83.4 (1.79)	82.4 (1.72)	81.2 (2.38)	79.8 (1.49)	80.1 (1.79)	91.2 (2.32)	92.3 (2.41)	91.2 (1.32)
×	√	×	84.5 (1.72)	83.1 (1.62)	82.6 (1.42)	81.1 (1.87)	79.3 (1.84)	78.9 (1.32)	92.6 (1.26)	92.7 (1.35)	92.6 (0.97)
×	×	√	86.9 (1.04)	85.6 (0.98)	85.6 (0.83)	82.5 (0.88)	81.2 (0.79)	81.4 (0.73)	96.4 (1.32)	93.6 (1.05)	95.0 (0.94)
√	√	×	84.7 (1.53)	83.2 (1.46)	82.7 (1.24)	81.3 (1.47)	79.4 (1.29)	78.9 (1.03)	92.9 (2.12)	91.7 (1.97)	91.6 (1.61)
√	×	√	87.1 (0.69)	85.1 (0.69)	86.1 (0.58)	82.0 (0.71)	81.2 (0.67)	81.7 (0.61)	97.1 (0.93)	96.2 (0.97)	97.3 (0.86)
×	√	√	90.0 (0.57)	85.8 (0.59)	87.4 (0.44)	87.0 (0.73)	84.8 (0.91)	83.6 (0.82)	94.1 (0.99)	90.1 (1.04)	93.2 (0.85)
√	√	√	90.1 (0.54)	86.2 (0.66)	88.7 (0.49)	87.2 (0.67)	83.1 (0.59)	83.2 (0.51)	94.1 (1.04)	92.2 (0.92)	95.1 (1.01)

Table 6: Average accuracy, precision, and recall (%) of our methods for the target encoder pre-trained on Tiny-ImageNet dataset. √ (or ×) means the inferrer has (or does not have) access to the corresponding background knowledge of the target encoder. The numbers in parenthesis are standard deviations in 5 trials.

Pre-training data distribution	Encoder architecture	Training algorithm	Accuracy			Precision			Recall		
			EncoderMI-V	EncoderMI-S	EncoderMI-T	EncoderMI-V	EncoderMI-S	EncoderMI-T	EncoderMI-V	EncoderMI-S	EncoderMI-T
×	×	×	88.7 (1.81)	84.9 (1.73)	85.3 (1.67)	86.0 (1.98)	81.5 (2.03)	81.8 (1.74)	90.1 (1.96)	95.3 (1.67)	95.9 (1.44)
√	×	×	93.0 (1.74)	88.2 (1.68)	90.0 (1.44)	90.1 (1.39)	85.4 (1.45)	86.8 (1.23)	97.8 (1.26)	93.2 (1.22)	97.1 (1.11)
×	√	×	89.1 (1.63)	86.4 (1.64)	85.7 (1.29)	83.3 (1.88)	84.0 (1.84)	80.1 (1.63)	96.3 (1.22)	91.1 (1.29)	96.1 (1.08)
×	×	√	94.1 (1.07)	91.3 (1.03)	94.1 (0.91)	90.7 (0.88)	90.3 (0.87)	93.5 (0.79)	97.4 (0.92)	91.3 (1.22)	95.6 (0.93)
√	√	×	94.4 (1.38)	90.4 (1.33)	91.5 (1.26)	97.4 (0.96)	94.1 (0.91)	93.8 (0.91)	90.8 (1.46)	87.1 (1.37)	89.4 (1.22)
√	×	√	96.1 (0.67)	91.6 (0.69)	94.1 (0.54)	93.8 (0.73)	90.4 (0.68)	94.2 (0.62)	97.6 (0.99)	92.3 (1.02)	95.7 (0.88)
×	√	√	94.5 (0.59)	91.8 (0.56)	92.0 (0.53)	92.3 (0.93)	94.4 (0.91)	94.1 (0.86)	96.7 (0.92)	90.6 (0.79)	92.7 (0.77)
√	√	√	96.5 (0.51)	92.0 (0.47)	94.3 (0.43)	96.6 (0.72)	92.9 (0.59)	94.9 (0.57)	97.0 (0.93)	92.4 (0.89)	93.2 (0.91)

Table 7: Accuracy, precision, and recall (%) of Baseline-E with 3×1 patches and 3×5 patches.

(a) 3 × 1 Patches

Pre-training dataset	Accuracy	Precision	Recall
CIFAR10	60.2	57.4	79.3
STL10	64.1	63.7	65.7
Tiny-ImageNet	65.8	68.2	59.5

(b) 3 × 5 Patches

Pre-training dataset	Accuracy	Precision	Recall
CIFAR10	50.8	50.6	62.9
STL10	55.8	55.5	59.3
Tiny-ImageNet	52.7	52.4	58.4

palm, pine, willow, bicycle, bus, motorcycle, pickup truck, train, lawn-mower, rocket, streetcar, tank, tractor.